CHARACTERISATION OF POLYIMIDES IN HIGH-TEMPERATURE SLIDING

Pieter Samyn[1]
Jan Quintelier[2]
Patrick De Baets[3]
Gustaaf Schoukens[4]

Abstract

Polyimides are used in tribological applications because of their high strength and thermal stability up to 310°C (long term) and 480°C (short term). After sintering, secondary transition temperatures do not occur up to the degradation point. The tribological characteristics of sintered polyimides are presently investigated for counterface bulk temperatures between 100°C and 260°C. Through the high stiffness and lack of softening, transfer mechanisms are different than those of traditional engineering polymers. No transfer film was observed at low temperatures, resulting in high friction ($\mu > 0.30$). For bulk temperatures above 180°C a sudden drop in friction was found towards $\mu < 0.30$, in accordance with the formation of a non-homogeneous transfer film consisting of plate-like particles. Wear rates are minimum for a bulk temperature of 140°C and progressively increase at higher temperatures. The evaluation of two temperature models for calculating bulk and flash temperatures indicates that the wear transition corresponds to flash temperatures above 180°C. Thermal analysis reveals that the 180°C transition temperature is explained by dehydration effects. The orientation of the polymer chains at the sliding surface is investigated by post-mortem Raman spectroscopy, pointing out that the C-N-C bonds in the molecular structure are progressively stretched along the sliding direction with higher sliding temperatures. However, at 180°C there is a reorganisation between the axial and the transverse orientation.

Key-words: Polyimide; Temperature; Raman spectroscopy.

This paper is submitted for the 60th Annual ABM Congress
July 25 – 28, 2005, Belo Horizonte, MG, Brazil
[1] *Reasearch Assistant, Ghent University – Laboratory Soete, Dept. Mechanical Construction and Production, St. Pietersnieuwstraat 41, B-9000 Gent, Belgium*
[2] *Reasearch Assistant, Ghent University – Laboratory Soete, Dept. Mechanical Construction and Production, St. Pietersnieuwstraat 41, B-9000 Gent, Belgium*
[3] *Professor, Ghent University – Laboratory Soete, Dept. Mechanical Construction and Production, St. Pietersnieuwstraat 41, B-9000 Gent, Belgium*
[4] *Professor, Ghent University – Department of Textiles, Technologiepark 907, B-9052 Zwijnaarde, Belgium*

Corresponding author: Pieter.Samyn@UGent.be

1 INTRODUCTION

The favourable use of polymer materials in dry sliding is indicated by their self-lubricating ability with limited material transfer from the one rubbing surface to the other that is induced by viscous flow of the polymer part. However, the practical application range of technical polymers as e.g. polyamides is limited because of their low thermal stability. Polyimides posses an extremely high thermal resistance and are therefore used in high-performance sliding applications, where superior mechanical, chemical and thermal properties are required. The high stiffness and fewer tendency for softening however results in a different transfer behaviour compared to e.g. UHMWPE, where the polymer chains are easily drawn and oriented. Pioneering research on the tribological behaviour of polyimides in film or bulk material has been performed by Fusaro [1] and Tewari and Bijwe [2], mainly under vacuum conditions used for space-applications. Although their studies show transitions in friction and wear mechanisms at higher sliding temperatures, the reasons for it remain difficult to illustrate and become more pronounced under atmospheric sliding conditions. A close examination of the polyimide transfer behaviour [3] and the worn polymer surfaces can provide additional information on the changes in the material's physical or chemical structure under sliding. An in-depth analysis of the variation in the polyimide structure after sliding has been rarely investigated by means of Raman spectroscopy [4]. Present research compares sliding of sintered polyimide SP-1 (Vespel) against high alloy 40 CrMnNiMo8 steel (C = 0.43 %, Si < 0.30 %, Mn = 1.50 %, Cr = 2.00 %, Mo = 0.20 %, Ni = 1.10 %, hardness 300 HB and surface roughness R_a = 0.10 µm) under free and controlled temperatures, related to orientation effects.

2 EXPERIMENTAL

2.1 Tribological Test Procedure

Friction and wear tests are done on a cylinder-on-plate configuration in a PLINT TE 77 reciprocating test rig. A line contact between a polyimide SP-1 cylinder (Ø 6 mm x 15 mm) and a fixed steel counterface (58 mm x 38 mm x 4 mm) is applied. The oscillating motion is provided by a motor connected to an eccentric mechanism for the adjustment of the stroke, presently chosen at 15 mm. The sliding frequency varies between 10 Hz and 40 Hz, corresponding to sliding velocities of 0.3 m/s, 0.6 m/s, 0.9 m/s and 1.2 m/s over a total sliding distance of 15 km. The normal load F_N is arbitrarily chosen at 100 N and 150 N. Contact conditions for the initial line contact are calculated in Table 1 according to the Hertz theories. When the normal load F_N is applied, an elastic deformation δ_H occurs with an increase in static contact surface A_s and a pressure distribution with peak and mean values.

Table 1. Contact conditions.

Normal load	P_{peak} (MPa)	P_{mean} (MPa)	A_s (mm^2)	δ_H (µm)
100 N	43	54	2.3	4.6
150 N	52	67	2.8	6.6

With progressing wear, the contact area increases while the pressure on the macro-contact falls down to values of 1 to 3 MPa for different normal loads. The variation of contact conditions with sliding distance is shown in Figure 1a, together with the on-

line registration of a friction and wear curve on SP-1 (100 N, 0.3 m/s) in Figure 1b. Running-in effects are attributed to the change from line contact to flat contact. Steady-state conditions with stable friction and constant wear rates occur after 250 µm wear depth, corresponding to a stabilisation in contact pressure. Friction and wear data mentioned below refer to steady-state conditions.

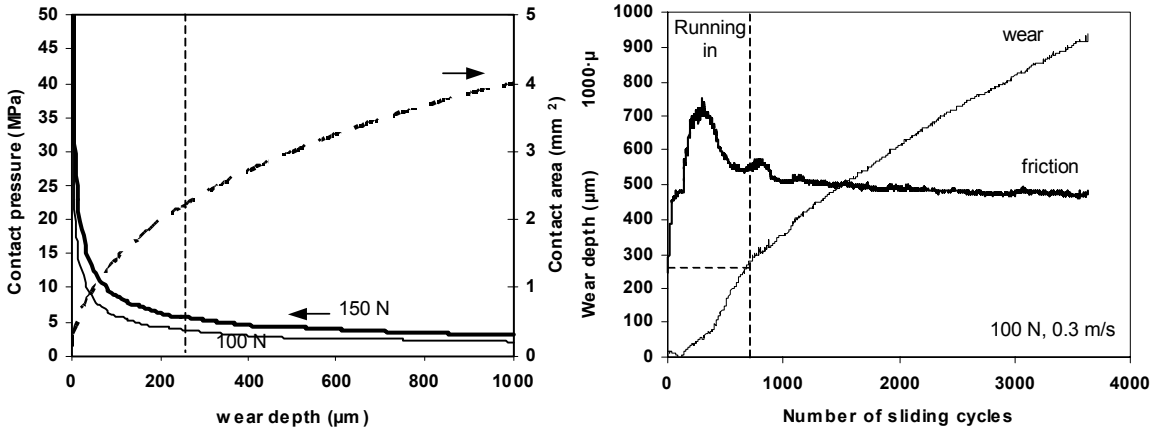

Figure 1. Variation of (a) contact conditions and (b) friction, wear with sliding distance.

A first series of tests is performed with free evolution of the contact temperature only resulting from frictional heating. Sliding temperatures are measured by a DIN 43710 K-type (nickel-chromium/nickel-aluminium) thermocouple positioned on top of the steel counterface 10 mm from the outer end of the sliding stroke. For a second series of tests, the load and sliding velocity are constant at 100 N or 150 N, 0.3 m/s while the steel counterface is heated at 100°C, 140°C, 180°C, 220°C and 260°C by four Vulstar heat cartridges (200 W, 400 W) positioned under the steel counterface.

2.2 Raman Spectroscopy

The polyimide surfaces are characterised by Raman spectroscopy after sliding under 100 N and 150 N at different temperatures. A Brucker FT spectrometer Equinox 55S (Bruker Optik, Ettlingen, Germany) is used, equipped with a Raman module FRA 106 fitted to a nitrogen cooled (77 K) germanium high sensitivity detector D418-T. The applied laser wavelength during the experiments was the 1.064 µm line from a Diode Laser Pumped Nd:YAG laser. All spectra are recorded at a resolution of 3 cm^{-1} using a non-focused laser beam with a power of 70 mW.

3 TEST RESULTS

3.1 Friction and Wear under Free Temperature

The coefficients of friction and wear rates measured under free contact temperature are shown in Table 2 for two normal loads and four sliding velocities. An increase in sliding velocity causes lower friction as generally expected from chain orientation, while an increase in normal load causes higher friction for 0.3 m/s to 0.9 m/s. This is caused by the lack of transfer formation under mild sliding conditions as discussed in [5]. A decrease in friction is only expected to occur under ‘thermally controlled’ conditions [6], however the onset of thermal controlled sliding shifts to higher sliding velocities when the normal load increases.

Table 2. Friction and wear of SP-1 under free temperature.

Sliding velocity (m/s)	100 N			150 N		
	Friction	Wear (10^{-4} mm^3/m)	Temperature (°C)	Friction	Wear (10^{-4} mm^3/m)	Temperature (°C)
0.3 m/s	0.48	20	61	0.53	75	78
0.6 m/s	0.39	38	86	0.45	25	118
0.9 m/s	0.36	35	110	0.38	56	145
1.2 m/s	0.39	33	122	0.32	69	160

The sliding temperatures as experimentally measured are referred to as bulk temperatures as they govern over the entire contact area. Experimental values are compared to the values theoretically calculated from the Loewen and Shaw model [7] according to formula (1). The heat input equals q = μpv (W/m^2) with μ the coefficient of friction, p the contact pressure and v the sliding velocity; ℓ is the semi-length in sliding direction, b is the semi-length perpendicular to the sliding direction and k_1 the thermal conductivity of the steel counterface (k_1 = 33 W/mK). Present model assumes that most of the heat is conducted into the steel specimen due to the low thermal conductivity of the polyimide sample (k_2 = 0.30 W/mK and thermal diffusivity a = 1.1 10^{-7} J/m^3/°C measured from DSC). A_{max} and A_{avg} are geometrical parameters calculated from the wear depth at steady-state as indicated in Figure 2 for estimation of a maximum and average bulk temperature.

$$\theta_{\max} = A_{\max}\frac{q\lambda}{k_1} \qquad \theta_{avg} = A_{avg}\frac{q\lambda}{k_1} \qquad (1)$$

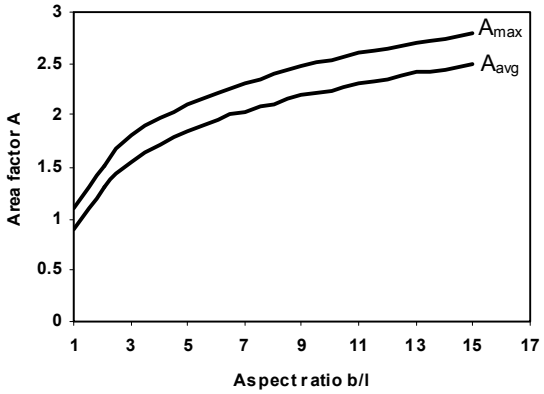

Figure 2. Loewen and Shaw model for calculation of bulktemperatures [7].

The flash temperature at the polyimide sliding surface is calculated from theories developed by Jaeger [8]. The general equation as given in Formula (2) has been implemented for two-dimensional contact with length *2ℓ* and width *2b* under contact pressure $p = F_N / (4b\,\ell)$. The temperature θ_f is superimposed on the bulk temperature for estimating the local maximum contact temperature.

$$\theta_f = 1.13\sqrt{\frac{\lambda a}{v}}\frac{\mu p v}{k_2} \qquad (2) \qquad\qquad \theta_f = 4.2\ 10^{-4}\frac{\mu\sqrt{v}\,F_N}{\sqrt{\lambda}\,b} \qquad (3)$$

Both temperature models are evaluated in Table 3, revealing that the experimentally measured bulk temperatures are in good agreement with the maximum bulk temperatures as calculated from Loewen and Shaw. The maximum flash temperature locally rises much higher due to the small fraction of real contact points where the heat is effectively conducted into the sliding bodies.

Table 3. Measured and calculated temperatures under free temperature.

Sliding velocity	100 N			150 N		
	θ avg	θ max	Maximum contact temperature (°C)	θ avg	θ max	Maximum contact temperature (°C)
0.3 m/s	53	58	89	70	77	126
0.6 m/s	71	79	111	99	114	172
0.9 m/s	86	108	128	114	137	177
1.2 m/s	116	129	172	127	177	188

Figure 3 shows the friction, bulk temperatures and wear rates as a function of the pv-parameter, showing a linear decreasing trend for the coefficients of friction and a linear increasing trend in wear rates for higher pv-values. However, there remains a relatively large scatter in test results, depending on the individual normal load or sliding velocity. Both parameters influence the contact temperature, although each of them affects the formation of an eventual transfer layer in a different way. An increase in sliding velocity is more favourable for lowering friction than an increase in load, since not only the sliding temperature is increased for higher sliding velocities, also the polymer chain orientation at the sliding surface become more pronounced.

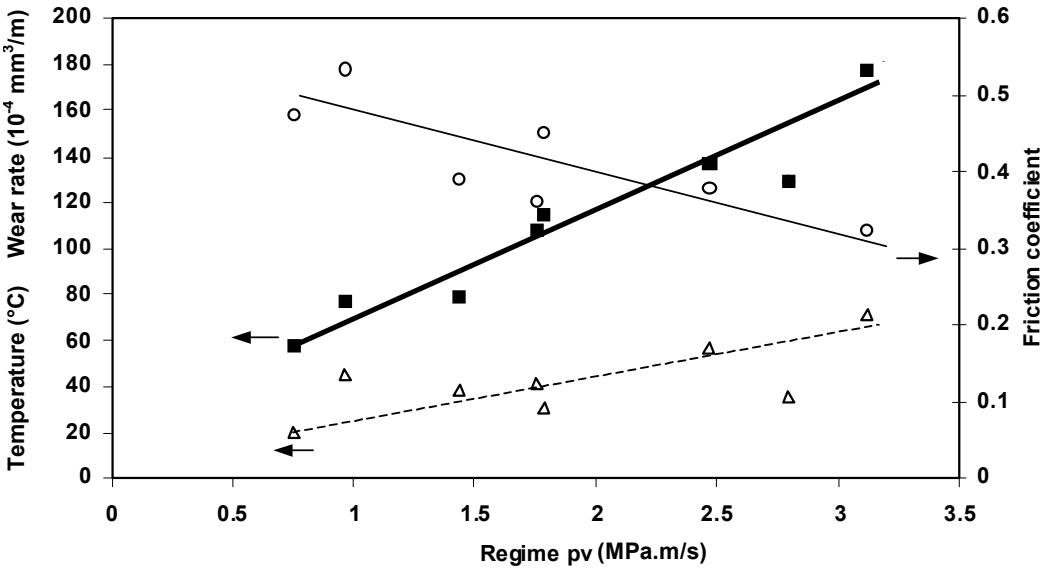

Figure 3. Influence of pv-parameter on friction (○), volumetric wear rate (Δ) and maximum bulk temperature (■) for sliding under free temperature.

3.2 Friction and Wear under Controlled Temperature

The evolution of friction with variable bulk temperatures under 100 N and 150 N is shown in Figure 4. They are averaged after 30 m and after 8000 m of sliding, revealing two regimes with a transition from high friction (μ = 0.40) towards low friction (μ = 0.30 to 0.20) at bulk temperatures above 180°C. Present transition is more evident than findings of Iwabuchi et al. [9] investigating SP-1 under fretting conditions. At ambient pressure of 10^5 Pa he observed slightly higher coefficients of friction above 200°C, although this trend diminished at the end of the sliding test

towards constant friction as a function of temperature. The significant difference between fretting and reciprocating sliding is that wear debris is not removed from the interface, permitting easy transfer of polyimide to an opposing surface. Under unidirectional sliding however, Tanaka and Ueda [10] found also higher steady-state coefficients of friction above 200 °C owing to the type of transfer.

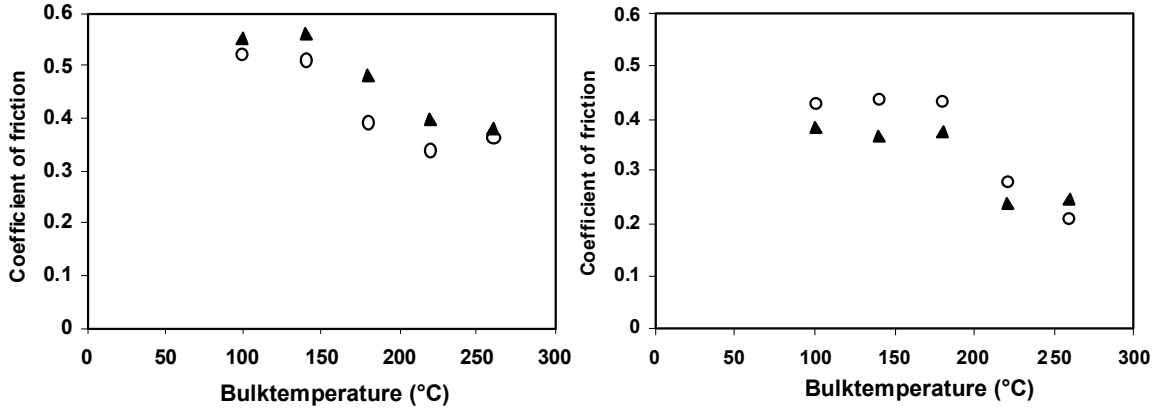

(a) **(b)**

Figure 4. Coefficients of friction under 100 N (▲) and 150 N (○) at 0.3 m/s for different temperatures, (a) after 30 m sliding, (b) after 8000 m sliding.

The flash temperatures and locally dissipated frictional energy (J/s) corresponding to each test under controlled bulk temperature is given in Table 4, with the maximum contact temperature calculated from the Jaeger model. It appears that the flash temperatures remain below the reported long-time exposure limit of 310°C. From measurements under free temperature (Table 3) and controlled temperature, it seems that the overall bulk temperature is more important than the local flash temperature for causing transitions in friction. The local maximum temperature in case of the 150 N, 140°C sliding test exceeds the friction transition temperature of 180°C although its coefficient of friction is still above 0.30, while a sliding test with bulk temperatures above 180°C readily causes strong decrease in friction.

Table 4. Calculated flash temperatures under controlled temperature

Bulk temperature	100 N			150 N		
	Semi-contact Length (mm)	Dissipated frictional energy (J/s)	Maximum contact temperature (°C)	Semi-contact Length (mm)	Dissipated frictional energy (J/s)	Maximum contact temperature (°C)
100 °C	1.93	11.55	127	2.28	19.35	141
140 °C	1.73	11.10	177	1.31	19.80	196
180 °C	2.04	11.25	205	1.87	19.35	227
220 °C	2.32	7.22	235	2.60	12.60	245
260 °C	2.24	7.51	276	2.14	9.54	281

The volumetric wear rates as calculated from weight measurements are given in Figure 5. In contrast to findings of Cong [11], reporting higher wear rates with increasing temperature for thermoplastic polyimides, the sintered polyimides (semi-thermosets) show minimum wear rate at 140°C. Under those sliding conditions it appears that the flash temperature attains 180°C, corresponding to local softening of the polyimide surface, although not able for transfer onto the counterface.

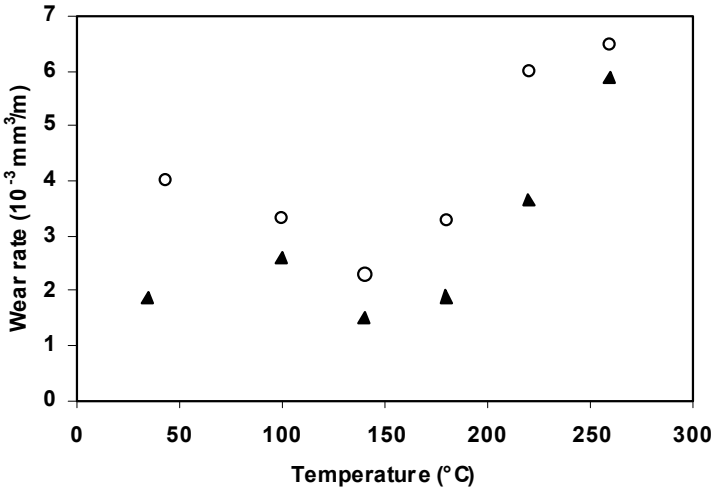

Figure 5. Wear rates for temperature controlled tests under 100 N (▲) and 150 N (○).

4 CHARACTERISATION OF POLYIMIDE SLIDING SURFACES

4.1 Thermal Stability

Unworn sintered polyimide samples are analysed by thermogravimetric (TGA) and Differential thermal analysis (DTA) measured in Figure 6a. Figure 6b shows a Differential Scanning Calorimetric (DSC) thermogram of SP-1. It is concluded from the DTA curve that an endothermic reaction occurs at 180°C, corresponding to dehydration effects. Dehydration processes are generally found to spread over somewhat large temperature intervals, resulting in broad temperature steps. At higher temperatures, no further transitions are found for SP-1, indicating its thermal stability up to 500°C. The reaction at 180°C corresponds to a mass loss registered by TGA and a different slope in heat capacity slightly revealed from DSC thermographs.

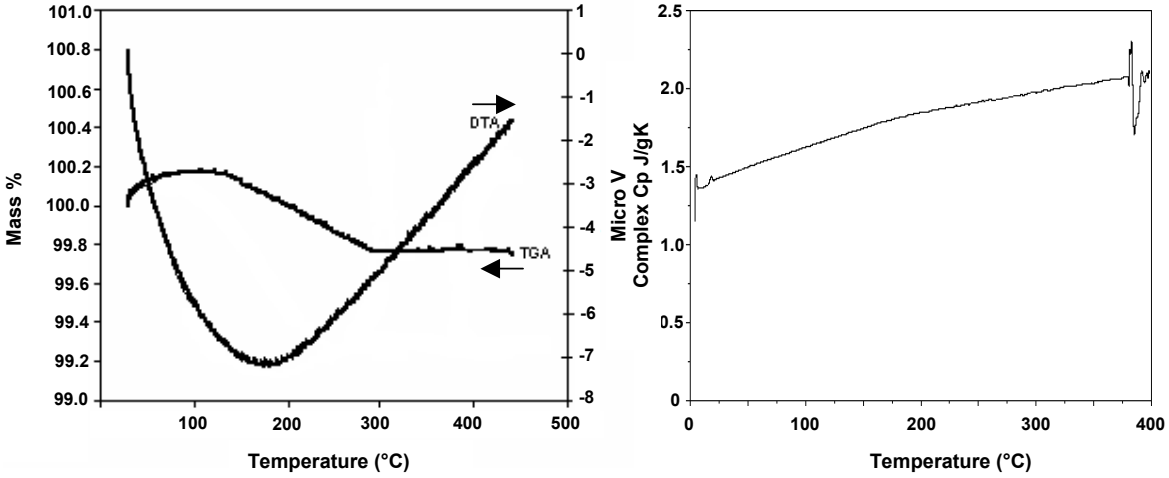

Figure 6. Thermal analysis of SP-1 by (a) TGA/DTA and (b) DSC

4.2 Transfer Film Formation

Figure 7 shows microscopic photos of both the steel and the polyimide wear surfaces. The steel surfaces after sliding under 200°C and 260°C are covered with a polyimide transfer film (A), gaining homogeneity at higher loads and temperatures.

Although in none of the cases a complete homogeneous and smooth film is observed due to the brittle nature of polyimides. This film is favourable for low friction, as there was no transfer film observed for bulk temperatures below 180°C. The polyimide surfaces show degradation as black spots (B) of unreacted polyimide precursor parts (cylinders are only 40% imidized) and a plastified film (C) on the surface above 180°C. Under lower temperatures, abrasive grooves parallel to the sliding direction and tearing of polyimide flakes out the surface are attributed to lack of plastification.

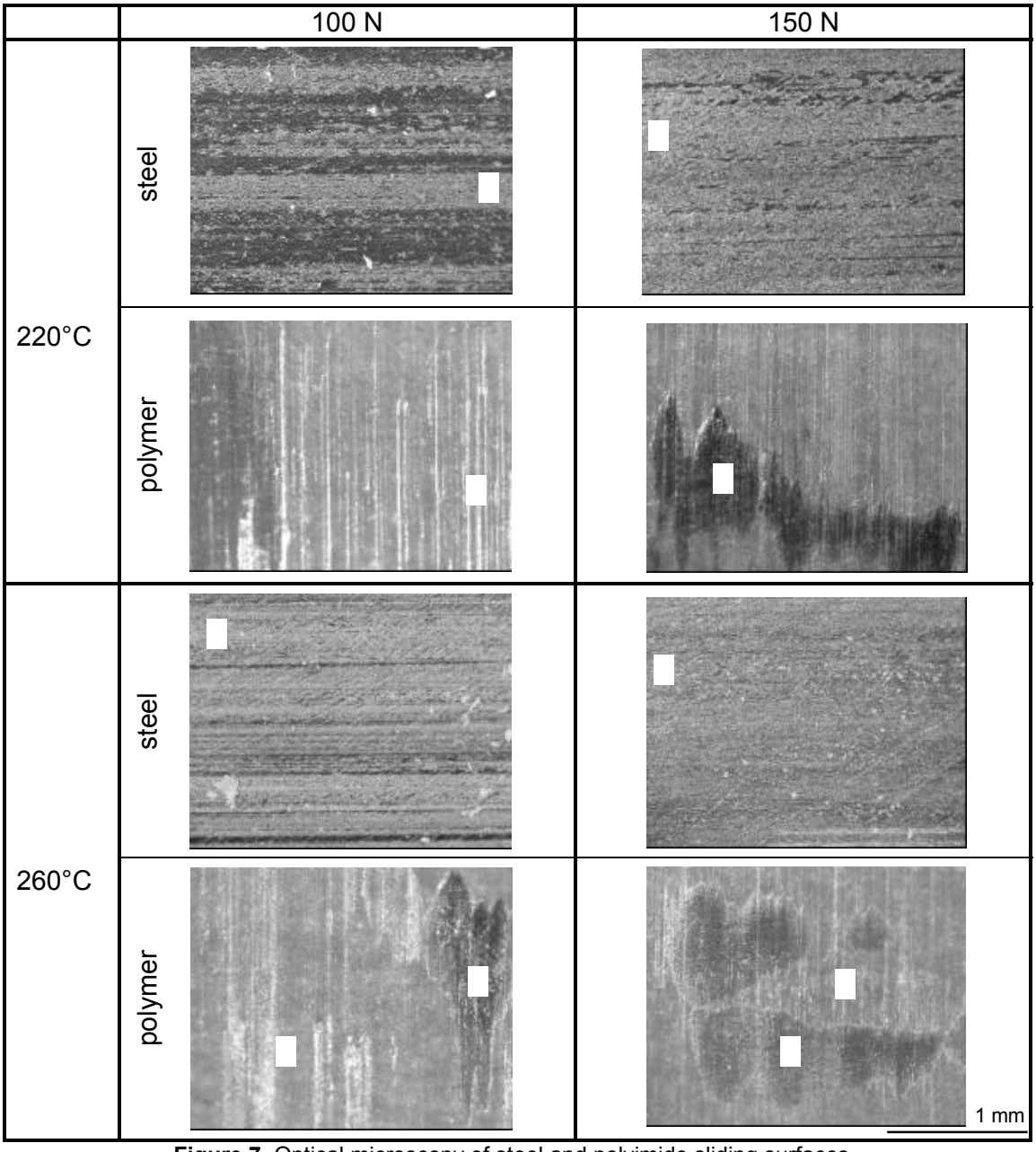

Figure 7. Optical microscopy of steel and polyimide sliding surfaces

4.3 Raman Spectroscopy

The Raman spectra taken from the worn polyimide surfaces are plotted in Figure 8 and Figure 9 for 100 N and 150 N normal loads respectively under different temperatures. The corresponding structure is given for some bands.

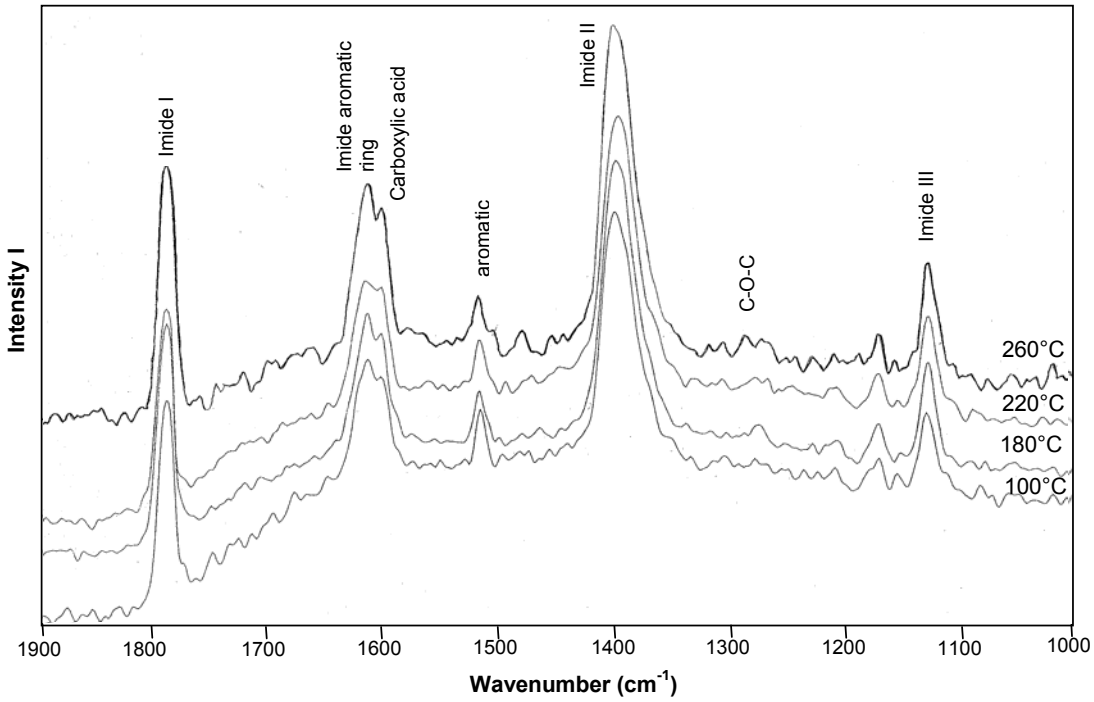

Figure 8. Raman spectra of SP-1 sliding under 100 N at different temperatures.

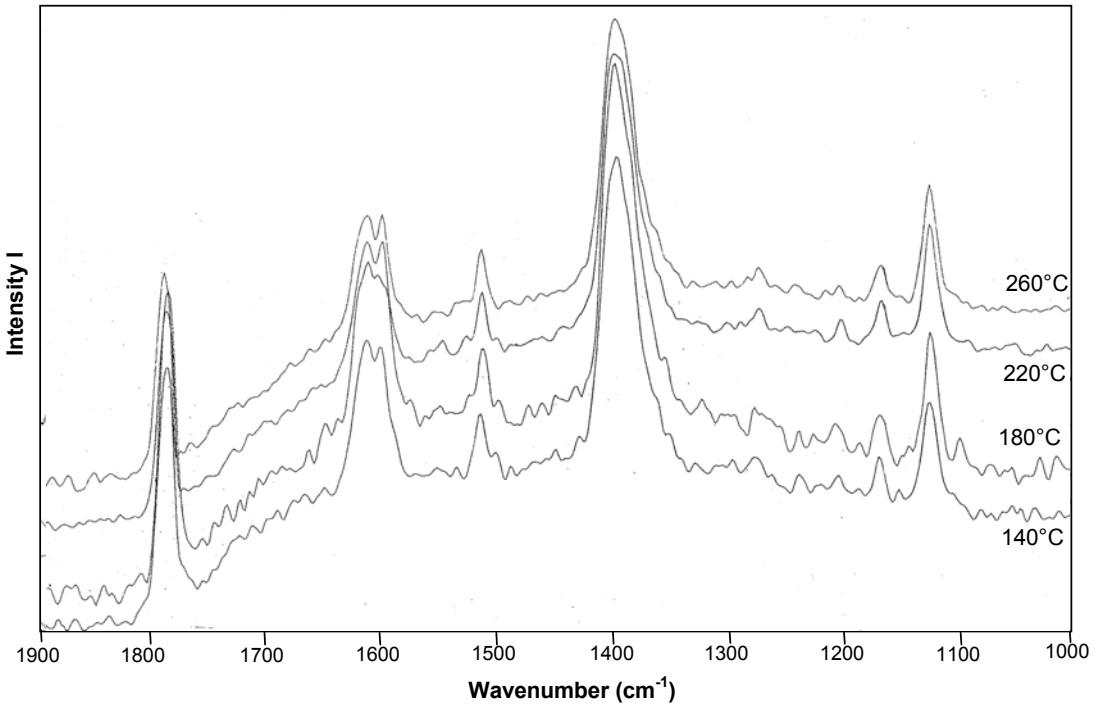

Figure 9. Raman spectra of SP-1 sliding under 150 N at different temperatures.

The orientation of the C-N-C imide bonds in the molecular structure is indicated by the 1124 cm^{-1} band. In Figure 10 the relative intensities of the 1124 cm^{-1}/ 1612 cm^{-1} and the 1124 cm^{-1} / 1395 cm^{-1} band is shown, calculated from the base-line method. It is concluded that the overall orientation increases with higher sliding temperatures in accordance with higher chain mobility, although there is a transition from the axial

orientation (represented by 1124 cm^{-1}) towards the transverse orientation (represented by 1395 cm^{-1}) at 180°C, indicated by a maximum value under 100 N.

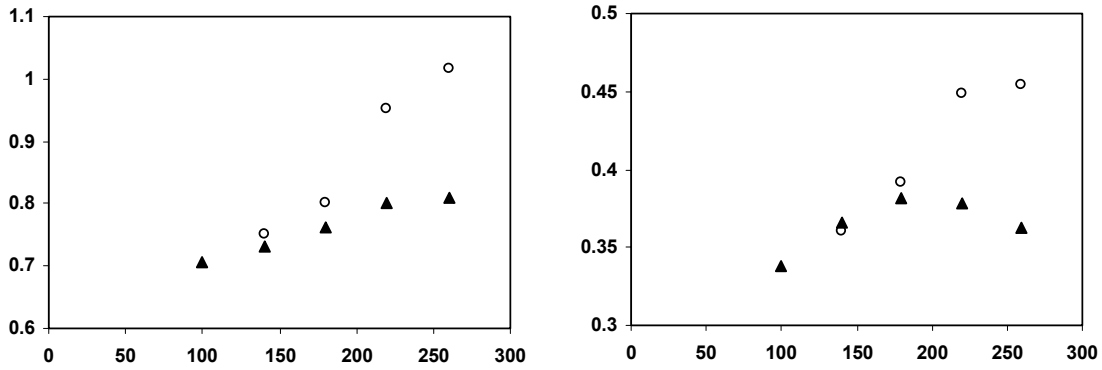

Figure 10. Relative intensities of absorption frequencies specific for C-N-C groups under 100 N (▲) and 150 N (○).

5. CONCLUSIONS

Sliding tests on sintered polyimides under free and controlled temperatures reveal a transition in friction at 180°C bulk temperatures. This corresponds to an endothermic reaction demonstrated by thermal analysis and reorientation of the C-N-C molecular structure, allowing for transfer. Temperature models however demonstrate that mainly the overall bulk temperature is important for transitions in friction, while a transition in wear behaviour is governed by the local flash temperature.

References

1 R.L. Fusaro, Trib. Trans., 31 Vol. 2 (1988), 174-181
2 U.S. Tewari, J. Bijwe, Tribological behaviour of polyimides, Marcel Dekker Inc. (1996), 533-583
3 S. Bahadur, Wear 245 (2000), 92-99
4 T.W. Sharf, I.L. Singer, Trib. Let, 14 Vol. 1 (2003), 3-8
5 P. Samyn, P. De Baets, G. Schoukens, B. Hendrickx, Pol. Eng. Sc., 43 No. 8 (2003), 1477-1487
6 C.M. McC. Ettles, ASLE Trans. 30, 2 (1987), 149-159
7 B. Bhushan, Principles and Applications of tribology, Wiley-Interscience (1999), New York, ISBN 0-471-59407-5
8 C.J. Jaeger, Proc. Roy. Soc., NSW 76 (1942), 1107-1121
9 A. Iwabuchi, K. Hori, Y. Sugawara, Wear 125 (1988), 67-81
10 K. Tanaka, S. Ueda, J. Jpn. Soc. Lubr. Eng., 26 (1980), 62
11 P.H. Cong, T.S. Li, X.J. Liu, X.S. Zhang, Q.J. Xue, Acta Pol. Sinica, 5 (1998), 556-561